Biological Psychiatry: Celebrating 50 Years

Archival Report

Microstructural Changes in Higher-Order Nuclei of the Thalamus in Patients With First-Episode Psychosis

Kang Ik K. Cho, Yoo Bin Kwak, Wu Jeong Hwang, Junhee Lee, Minah Kim, Tae Young Lee, and Jun Soo Kwon

ABSTRACT

BACKGROUND: Disruption in the thalamus, such as volume, shape, and cortical connectivity, is regarded as an important pathophysiological mechanism in schizophrenia. However, there is little evidence of nuclei-specific structural alterations in the thalamus during early-stage psychosis, mainly because of the methodological limitations of conventional structural imaging in identifying the thalamic nuclei.

METHODS: A total of 37 patients with first-episode psychosis and 36 matched healthy control subjects underwent diffusion tensor imaging, diffusion kurtosis imaging, and T1-weighted magnetic resonance imaging. Connectivity-based segmentation of the thalamus was performed using diffusion tensor imaging, and averages of the diffusion kurtosis values, which represent microstructural complexity, were estimated using diffusion kurtosis imaging and were compared in each thalamic nucleus between the groups.

RESULTS: The mean kurtosis values in the thalamic regions with strong connections to the orbitofrontal cortex ($F_{1,70} = 8.40$, $p < .01$) and the lateral temporal cortex ($F_{1,70} = 8.46$, $p < .01$) were significantly reduced in patients with first-episode psychosis compared with those of the healthy control subjects. The mean kurtosis values in the thalamic region with strong connection to the orbitofrontal cortex showed a significant correlation with spatial working memory accuracy in patients with first-episode psychosis ($r = .36$, $p < .05$), whereas no significant correlation between these variables was observed in the healthy control subjects.

CONCLUSIONS: The observed pattern of reduced microstructural complexity in the nuclei not only highlights the involvement of the thalamus but also emphasizes the role of the higher-order nuclei in the pathophysiology beginning in the early stage of schizophrenia.

Keywords: Diffusion-weighted, Mediodorsal nucleus, Multimodal, Pulvinar nucleus, Schizophrenia, Thalamus

https://doi.org/10.1016/j.biopsych.2018.05.019

Clinical symptoms and cognitive impairments are heterogeneous in patients with schizophrenia. This has led to the pursuit of discovering more specific genetic and biological markers that underlie the pathophysiology of schizophrenia. The thalamus is one of the brain regions most affected in schizophrenia, and there have been reports of various defects in this region, such as a reduced number of neurons (1,2), reduced volume (3–6), altered neurochemistry (7,8), and abnormal brain activation (9–12). Consequently, characterizing thalamic defects and models of the pathophysiology involving the thalamus, such as Andreasen's cognitive dysmetria (13), has drawn attention in schizophrenia research. Furthermore, fairly consistent reports of reduced structural and functional connectivity between the thalamus and the prefrontal cortex and increased connections between the thalamus and the parietal/somatomotor cortices in schizophrenia (14–20) strongly highlight the role of the thalamus in the pathophysiology of schizophrenia.

The thalamus is composed of nuclei, each having different cytoarchitecture and connections (21). There have been investigations of the nuclei-specific alterations in schizophrenia, and most of the related evidence has come from postmortem investigations. As summarized well in the extensive review of the postmortem studies of the thalamus by Dorph-Petersen and Lewis (22), although large inconsistencies remain, the mediodorsal, anterior, and pulvinar nuclei are the most frequently reported thalamic nuclei with altered numbers of neurons (1,23) and volumes in schizophrenia (24,25). These nuclei constitute the higher-order nuclei, which have prominent connections to the prefrontal and temporal cortices. These findings align well not only with the most frequently reported morphometric and functional changes in the prefrontal and temporal cortices but also with the previously mentioned alterations in the thalamocortical connections in schizophrenia. Additionally, lesions of higher-order thalamic nuclei have been shown to impair a number of cognitive functions, including

SEE COMMENTARY ON PAGE 10

 ISSN: 0006-3223

memory, attention, perception, and sensory-guided actions (26–28). Furthermore, recent evidence suggests that higher-order thalamic lesions disturb corticocortical information transmission (29,30). These findings highlighted the possible involvement of the higher-order nuclei of the thalamus in the pathophysiology of schizophrenia and the need for their investigation.

However, there are inevitable limitations to the postmortem investigations of the thalamic nucleus. Not only is it extremely difficult to collect an adequate number of samples in early adulthood, but also there are highly confounding effects that arise from the lifelong impact of the disorder, such as effects of medications. In vivo magnetic resonance imaging approaches could overcome many of the limitations existing in the postmortem method, as these approaches could measure the changes in the early stage of the disorder (31,32). Kemether *et al.* reported volume reductions in the centromedian, mediodorsal, and pulvinar nuclei (33) in patients with schizophrenia. This study provides one example of a noninvasive neuroimaging approach for investigating the thalamus at the level of the nuclei, and it found a pattern consistent with that of postmortem findings. However, there remains a need for investigating the thalamic nuclei using more advanced methods for characterizing thalamic nuclei with more detail, to which multimodal neuroimaging could offer its advantages. More recent approaches using diffusion tensor imaging have allowed segmentation of the thalamus based on voxel connectivity (34–36), and Kim *et al.* compared the volumes of the thalamic segments in schizophrenia using anatomical connectivity-based segmentation (37). Consistent with the previous findings from postmortem investigations, a reduction in the volume of the thalamic region that has the most connections to the orbitofrontal cortex, namely, the mediodorsal nucleus, was reported. However, the investigation of thalamic-segment volumes using connectivity-based segmentation rests on the assumption that the thalamocortical connectivity pattern is preserved. This assumption may be unwarranted in schizophrenia, as there have been plenty of reports of altered connectivity, as previously mentioned. Therefore, a multimodal approach is needed to complement this limitation.

Investigation of microstructure may provide additional information regarding the volume of the regions identified by connectivity-based segmentation. Generally, the volume measurement depends on the boundaries of different structures. Although the measure is very useful and easy to interpret, there exists the possibility of subtle microstructural changes that do not cause detectable alterations in the structural boundaries, such as changes in macromolecule concentrations and the proliferation of cell membranes and organelles. Therefore, volume measurements would be limited in detecting these microstructural changes. By investigating the microstructure within the thalamic segments with high probabilities of connection, which may represent the core regions of the segment, more of the intrinsic changes could be revealed in a way that is less dependent on the segmentation method based on the connectivity.

As a descriptor of a probability distribution, kurtosis is a measure of the "tailedness" of a probability distribution. Diffusion kurtosis imaging (DKI), which is a relatively new measure within the neuroimaging field, quantifies the deviation of the water-diffusion profile from a Gaussian distribution, potentially allowing sensitivity to underlying microstructural barriers undetected by the standard diffusion tensor metrics (38). The microstructural complexity measured by DKI may refer to the overall microstructural changes, including changes in soma size, oligodendrocyte density, dendritic spine length and density, and neuronal cell density (39–41). Figure 1 shows the relationship between diffusion kurtosis and microstructural changes. This approach could add additional information to the state of microstructural anomalies in the thalamic nuclei. Consistent with the findings of a rodent study by Cheung *et al.* (42), Paydar *et al.* reported a gradual increase in mean kurtosis (MK) in humans from birth to approximately 4 years of age, where the changes were detected not only in white matter but also in the isotropic gray matter regions, including the thalamus (43). A progressive increase in macromolecule concentrations, proliferation of cell membranes and organelles, the transition of radial glial cells to astrocytic neuropils, the addition of basal dendrites, and cell packing were speculated as possible reasons for the MK increase. These factors are possibly related to defective changes in schizophrenia, as it is a disorder of a neurodevelopmental nature. However, the state of the microstructural complexity in the thalamus and its nuclei in patients with schizophrenia has not yet been reported yet.

Additionally, with patients with chronic illness, it would be difficult to conclude that the thalamic changes occur early in the disorder. Therefore, we aimed to investigate the microstructural changes in patients with first-episode psychosis (FEP). This approach minimizes the long-term effects of the disorder, such as the effects of medication, poor diet, less exercise, or heavy smoking.

It is hypothesized that the patients with FEP will show reduced thalamic microstructural complexity in the mediodorsal and pulvinar nuclei, which would be represented by reduced MK. We hope to highlight the importance of the early nuclei-specific alterations in the pathophysiology of schizophrenia.

METHODS AND MATERIALS

Thirty-seven patients with FEP were selected, between April 2010 and June 2014, from a slightly larger pool of patients who visited Seoul National University Hospital for their symptoms and agreed to participate in the research. Intensive clinical interviews were conducted for all patients with FEP by experienced psychiatrists, using the Structured Clinical Interview for DSM-IV-TR Axis I Disorders (SCID-I) to identify past and current psychiatric illnesses. The inclusion criteria were age between 15 and 40 years and diagnosis of brief psychotic disorder, schizophreniform disorder, schizophrenia, or schizoaffective disorder following the DSM-IV criteria. Furthermore, the duration of illness had to be $<$1 year. Participants were excluded from the study if they had intellectual disability, history of substance use disorder, head trauma with loss of consciousness, seizure, meningitis, neurosurgical operation, or any other clinically significant medical illness. Of the patients with FEP, 31 were receiving antipsychotics at the time of scanning, and of these patients, 3 were taking typical antipsychotics while the others were taking atypical antipsychotics. The average daily dose of antipsychotics in a chlorpromazine equivalent dose (44) and the average duration of medication use are in Table 1. Among the patients, 4 were

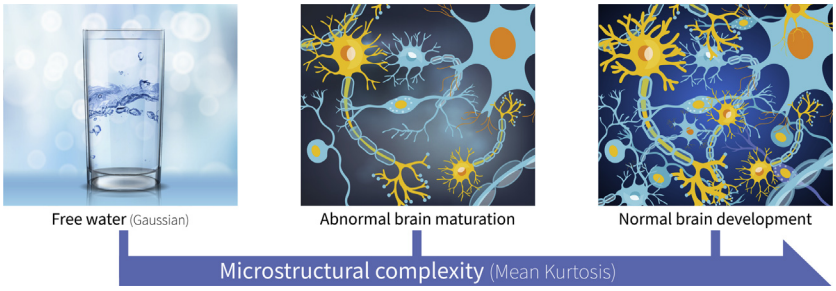

Figure 1. Schematic summary of the microstructural complexity investigated with mean kurtosis values. Free water has a Gaussian distribution of the displacement profile, which makes the kurtosis value zero. However, as brain tissues develops, thus increasingly occupying space and hindering diffusion, the diffusion profile becomes more complicated and deviates from the Gaussian distribution. This results in increased kurtosis values.

on antidepressants, and 20 were on anxiolytics. All included patients were Korean, and their primary clinical setting at the time of recruitment was inpatient for 15 individuals and outpatient for the others.

The Positive and Negative Syndrome Scale (45) and the Global Assessment of Functioning Scale (46) were administered to the patients with FEP.

In addition, 36 healthy control subjects (HCs), matched for age, gender, and education level, were recruited through Internet advertisements. The exclusion criteria for HCs included past or current diagnosis of an Axis I disorder via Structured Clinical Interview for DSM-IV-TR Axis I Disorders Nonpatient Edition and any first- to third-degree biological relative with a psychiatric disorder. Informed written consent was obtained from all participants, and the study was conducted in accordance with the Declaration of Helsinki. The study was also approved by the institutional review board of the Seoul National University Hospital. To estimate the IQs of the patients, an abbreviated form of the Korean version of the Wechsler Adult Intelligence Scale (47) was administered to all participants.

Neuropsychological Assessment

The cognitive functions that were previously reported to involve the thalamus, such as working memory, attention, and verbal fluency were tested using the spatial working memory (SWM) task in the Cambridge Neuropsychological Test Automated Battery, Trail Making Test, Wisconsin Card Sorting Test, and Controlled Oral Word Association Test (48). The number of participants with neuropsychological assessment data for each test is included in the Supplement.

Image Acquisition

T1-weighted diffusion tensor imaging and DKI data were acquired using a 3T scanner (Magnetom Trio; Siemens, Erlangen, Germany). T1-weighted images were acquired using a three-dimensional magnetization prepared rapid acquisition gradient-echo sequence with the following parameters: repetition time 1670 ms, echo time 1.89 ms, voxel size 1 mm^3, 250 mm field of view, 9° flip angle, and 208 slices. Diffusion-weighted images were acquired using echo-planar imaging in the axial plane with the following parameters: repetition time 11,400 ms, echo time 88 ms, matrix 128 × 128, field of view 240 mm, and voxel size 1.9 × 1.9 × 3.5 mm^3. Diffusion-sensitizing gradient-echo encoding was applied in 64 directions using a diffusion-weighting b factor of 1000 s/mm^2. One volume was acquired with a b factor of 0 s/mm^2 (B0). Diffusion kurtosis images were acquired using echo-planar imaging with the following parameters: repetition time 5900

Table 1. Demographic and Clinical Characteristics of the Participants

Variable	Patients With FEP (n = 37)	HCs (n = 36)	χ^2 or t	p
Age, Years, Mean ± SD	22.4 ± 5.5	23.5 ± 6.0	0.82	.42
Gender, Male/Female, n	16/21	17/19	0.01	.92
IQ	97.3 ± 13.8	105.5 ± 10.4	2.86	.01[a]
Handedness, Right/Left, n	31/6	35/1	2.41	.12
Education, Years, Mean ± SD	13.1 ± 2.1	13.8 ± 1.6	1.54	.13
Parental SES Score, Mean ± SD	2.9 ± 0.4	3.0 ± 0.2	1.01	.31
Duration of Illness, Mo, Mean ± SD	5.9 ± 3.8			
Medication Dose, CPZ Equivalent, mg, Mean ± SD	195.7 ± 210.2			
PANSS Score, Mean ± SD				
Total	68.6 ± 13.3			
Positive	16.3 ± 5.0			
Negative	17.4 ± 5.3			
General	34.9 ± 7.0			
GAF Score, Mean ± SD	46.2 ± 10.8			

CPZ, chlorpromazine; FEP, first-episode psychosis; GAF, Global Assessment of Functioning Scale; HCs, healthy control subjects; PANSS, Positive and Negative Syndrome Scale; SES, socioeconomic status.

[a]This p value is statistically significant.

ms, echo time 190 ms, and the same matrix size, field of view, voxel size, and number of B0 as diffusion tensor imaging, with 30 diffusion gradient directions each using five diffusion-weighting b-factor values: 500, 1000, 1500, 2000, and 2500 s/mm^2.

Magnetic Resonance Image Processing

T1-Weighted Imaging. Cortical regions of interest (ROIs) in each individual's T1 space were automatically selected as binary masks using FreeSurfer (49). Each side of the cortex was divided into eight ROIs in accordance with previous studies (17,50): orbitofrontal cortex (OFC), lateral prefrontal cortex, medial prefrontal cortex, lateral temporal cortex (LTC), medial temporal cortex, somatomotor cortex, parietal cortex, and occipital cortex.

Diffusion-Weighted Imaging. The diffusion-weighted imaging data were preprocessed using eddy-current correction, skull removal, and motion correction with FSL (51). Information about the quality assurance is included in the Supplement. Individual B0 images were used as a reference in registering their own T1 images to the diffusion space, creating transformation matrices that were used to bring the ROIs into the diffusion space. FLIRT (52,53) was used for this registration, with a mutual information cost function and trilinear interpolation. Then, for each side of the brain, FSL probabilistic tractography (54) was applied with the default options of the probtrackx2 (number of samples, 5000; number of steps per sample, 2000; step length, 0.5 mm; and curvature threshold, 0.2) using the ROI of the thalamus as a seed and the eight cortical ROIs as targets.

Connectivity-Based Segmentation

The output from the probabilistic tractography included connectivity maps that contained a set of values for every voxel of the thalamus, representing the number of tractography samples that arrived at their target cortical ROIs (out of the 5000 initially seeded). These connection maps were divided by 5000 to create probability maps that represent the probability of connection between the seed and each cortical target (50,54). The thalamic-segment ROIs for the microstructural investigation were obtained by thresholding the probability maps to each cortex using the 90th percentile of the connectivity distribution. This step obtained the core thalamic segments with strong connections. The ROIs for the investigation were estimated in the subject space, which avoids warping distortions that may occur during registration to a common space. For visualization purposes, the probability maps of all participants were nonlinearly registered to the Montreal Neurological Institute space using FNIRT (55), averaged, and thresholded using the 90th percentile (Figure 2).

DKI: MK Calculation

The DKI data were eddy-current corrected and motion corrected using FSL (51). The Diffusion Kurtosis Estimator (56) was used with constrained linear weighting to calculate the MK image for each participant. After matching the space using FLIRT, the MK was estimated in each thalamic-segment ROI. Additionally, to visually and quantitatively show the thalamic nuclei that each thalamic-segment ROI with a significant MK change was similar to, the thalamic-segment ROIs from all participants were registered and overlaid on the Talairach atlas thalamic labels (57) and Behrens' thalamic atlas (34), estimating the percentage overlaps in Figure 5 (overlap with the Behrens labels is included in the Supplement).

Statistical Analysis

All statistical analyses were performed using R version 3.0.2 and SciPy version 0.14.0 (58,59). The demographics were tested for differences between patients with FEP and HCs using independent *t* tests and tests of equality of proportions. The results are summarized in Table 1.

The MKs of the thalamic-segment ROIs were tested with analyses of covariance (ANCOVAs) to reveal the group effect on MK, with age as a covariate. The results from the ANCOVAs were corrected for multiple comparisons using the false discovery rate correction. Then, the MKs in the thalamic-segment ROIs with significant group differences were tested for correlations with clinical scales, such as the Positive and Negative Syndrome Scale and the Global Assessment of Functioning Scale, and with neurocognitive tests, using Spearman's correlation analysis.

Supplementary Statistical Analysis

The thalamocortical connectivity of the thalamic regions that showed significant group differences in the MKs was estimated and tested for group differences using *t* tests after we controlled for the whole thalamocortical connectivity (17,50).

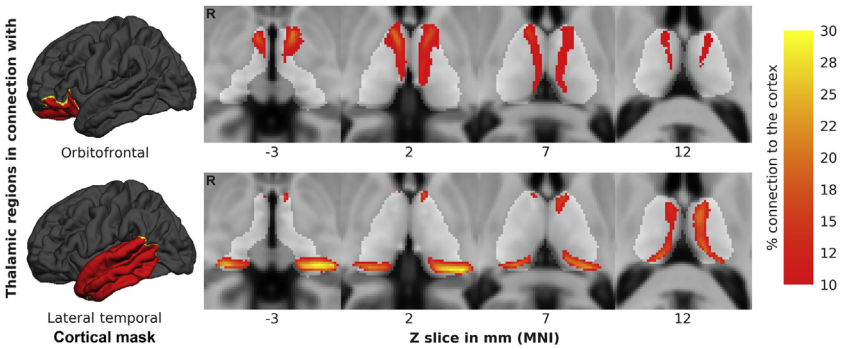

Figure 2. Visualization of the thalamic regions with strong connections to the orbitofrontal and lateral temporal cortices. Probabilistic maps of all subjects were registered to the Montreal Neurological Institute (MNI) space. The colors of the thalamic regions represent the average percent connection to their target cortex. R, right hemisphere.

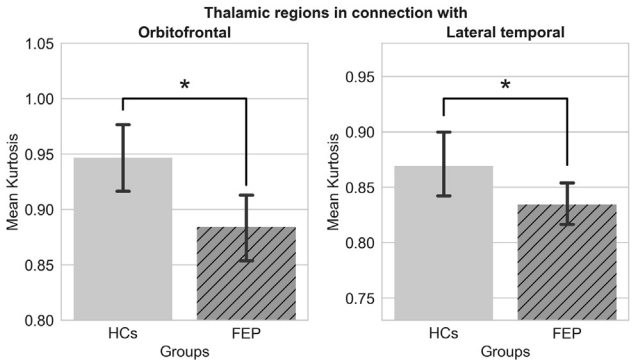

Figure 3. The mean kurtosis values in the thalamic regions with strong connections to the cortices for each group. The error bars represent the 95% confidence intervals. *Significant group effect after multiple comparison correction. FEP, patients with first-episode psychosis; HCs, healthy control subjects.

Correlations between MKs and connectivity were tested using Spearman's correlation analysis. Exploratory ANCOVAs for testing group effect on MK with the connectivity as a covariate were performed to identify group effect independent of the thalamocortical connectivity. Additionally, to further localize the microstructural abnormalities in patients with FEP, a voxelwise analysis of the MK maps was performed. Details of these analyses are included in the Supplement.

RESULTS

There were no significant differences in the demographic backgrounds between the patients with FEP and the HCs, except for their IQ scores (t_{71} = 2.86, $p < .05$) (Table 1).

The results of ANCOVA of the MKs are summarized in Table 2. There was a significant group effect on the MKs, in which patients with FEP exhibited reduced MKs in the thalamic ROIs with the strongest connections to the OFC ($F_{1,70}$ = 8.40, $p < .01$) and the LTC ($F_{1,70}$ = 8.46, $p < .005$). The group effect on other thalamic nuclei did not survive multiple-comparisons correction. The results are shown as a bar graph in Figure 3.

The MK in the thalamic region with strong connections to the OFC showed a significant correlation with SWM accuracy in patients with FEP (r = .36, $p < .05$) (Figure 4), whereas that of the HCs remained nonsignificant. MK in the thalamic region with strong connections to the LTC and other neurocognitive tests showed no significant correlations in each group. Additionally, the MKs of both thalamic regions were not significantly correlated with the Positive and Negative Syndrome Scale or the Global Assessment of Functioning Scale.

As shown in Figure 5A and B, the Talairach nuclei that had the most overlap with the thalamic segments with strong connections to the OFC and LTC were the medial dorsal (52%) and pulvinar (71%) nuclei.

Supplementary Analyses

The connection between the thalamus and the OFC was significantly reduced in the patients with FEP compared with that in the HCs (t_{71} = 2.02, $p < .05$); however, the connection with the LTC showed no significant difference between case and control groups (t_{71} = −0.45, $p > .05$). The connectivity between the thalamus and the LTC and the MK in the thalamic region with strong connections to the LTC showed a significant negative correlation (r = −.70, $p < .001$) in the HCs and a negative trend in the patients with FEP (r = −.29, p = .08).

Detailed information of the other analyses is included in the Supplement.

DISCUSSION

To our knowledge, this is the first study to report nuclei-specific microstructural alterations in the thalamus of patients with FEP. Our results revealed significantly reduced microstructural complexity in the thalamic regions with strong connections to the OFC and LTC in patients with FEP. By using measures of microstructure in vivo, our results could show that the nuclei-specific abnormalities in the thalamus exist from the early stages of the disorder, findings that have been somewhat elusive. Our results not only extended those of previous postmortem reports of the structural alterations in the thalamic nuclei (1,23–25) but also highlighted the possibility of defective developmental changes in schizophrenia.

Mediodorsal Nucleus

From the connectivity-based segmentation, the thalamic region with strong connections to the OFC lies in the

Table 2. Summary of the Comparisons of the Mean Kurtosis Values in the Thalamic Regions

Cortical Region to Which the Thalamic Region Has the Strongest Connection	HCs, Kurtosis Value, Mean ± SD	Patients With FEP, Kurtosis Value, Mean ± SD	F	p	FDR-Corrected p
LPFC	0.96 ± 0.08	0.92 ± 0.10	2.49	.119	.190
LTC	0.87 ± 0.10	0.80 ± 0.09	8.46	.005	.020[a]
MPFC	1.01 ± 0.10	0.99 ± 0.13	0.55	.460	.526
MTC	0.85 ± 0.11	0.79 ± 0.10	5.70	.020	.053
OCC	0.87 ± 0.07	0.84 ± 0.07	3.92	.052	.103
OFC	0.97 ± 0.10	0.88 ± 0.09	8.40	.005	.020[a]
PC	0.95 ± 0.09	0.95 ± 0.11	0.01	.940	.940
SMC	1.04 ± 0.12	1.02 ± 0.16	0.57	.453	.530

FDR, false discovery rate; FEP, first-episode psychosis; HCs, healthy control subjects; LPFC, lateral prefrontal cortex; LTC, lateral temporal cortex; MPFC, medial prefrontal cortex; MTC, medial temporal cortex; OCC, occipital cortex; OFC, orbitofrontal cortex; PC, parietal cortex; SMC, somatomotor cortex.

[a]FDR-corrected $p < .05$.

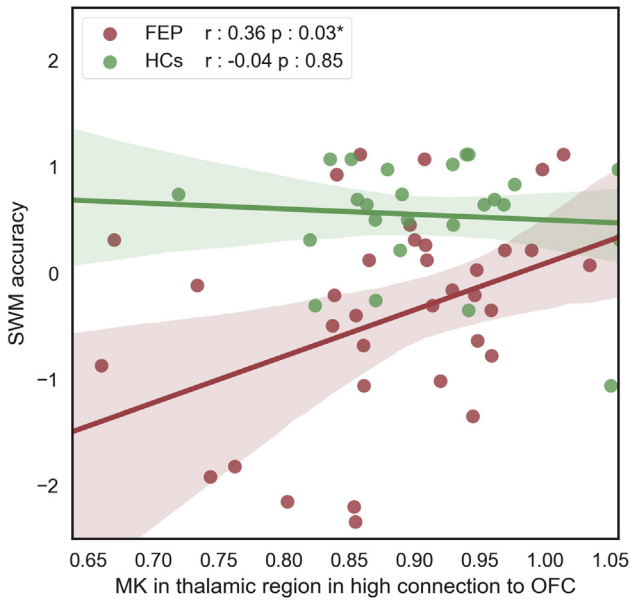

Figure 4. Correlation between the mean kurtosis (MK) values in the thalamic region with strong connections to the orbitofrontal cortex (OFC) and the spatial working memory (SWM) accuracy in each group. *$p < .05$. FEP, patients with first-episode psychosis; HCs, healthy controls.

mediodorsal region (Figure 2, upper row). As shown in the overlap analysis with the Talairach thalamic labels, this thalamic segment had the greatest overlap with the mediodorsal nucleus (Figure 5A and B, upper row). The mediodorsal nucleus is one of the higher-order thalamic nuclei, and it is heavily interconnected with the prefrontal cortex and the thalamic reticular nucleus, suggesting its role in signal transmission and control. The significant reduction in the MK in this region was consistent not only with the findings of reductions in the number of neurons and volumes in schizophrenia in previous postmortem studies (25,60,61) but also with the findings in previous reports of spindle deficits in schizophrenia (62–64). The microstructural changes in the mediodorsal nucleus have been speculated to result in disrupted signal transmission to the prefrontal cortex as well as to the thalamic reticular nucleus.

On the other side of the network, there lies the OFC, which has been shown to exhibit structural abnormalities in volume, cortical thickness, and sulcogyral patterns (65–67). The OFC is involved in emotion processing and in various higher-order cognitive functions, such as social cognition and decision making (68). On top of the reduced thalamo-OFC connectivity revealed by our supplementary analysis, the microstructural defects within the thalamic nuclei provide additional information about the reduction in the local microcircuitry and about the long-range connections that coexist in the mediodorsal nucleus in schizophrenia.

The mediodorsal nucleus also has connections to the limbic system, a finding that has been amply reported in regard to the abnormalities in schizophrenia (69–72). In line with this finding, the significant correlation between the microstructural complexity in the thalamic region with strong connections to the OFC and the SWM in FEP is consistent with the findings of previous reports of the involvement of the ventral midline nucleus of the thalamus in SWM (69,70). Microstructural abnormalities in this thalamic region are thought to perturb the prefrontal cortex–hippocampal network, which directly results in deficits in SWM in FEP.

Pulvinar Nucleus

The pulvinar nucleus is the thalamic region with the strongest connection to the LTC, which is located around the more superior medial boundary of the thalamus and extends

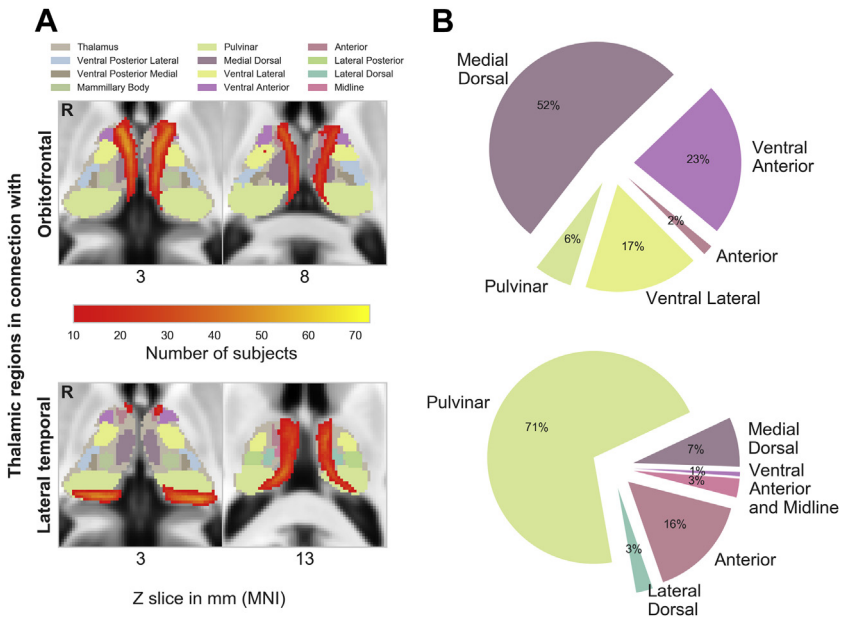

Figure 5. The top row represents information regarding the thalamic region with strong connections to the orbitofrontal cortex, and the bottom row represents information regarding the thalamic region with strong connections to the lateral temporal cortex. Panel **(A)** shows the thalamic regions strongly connected to each cortex overlaid on the Talairach thalamus nuclei labels. Panel **(B)** contains pie charts of the overlap between the thalamic regions with the Talairach thalamus nuclei labels. MNI, Montreal Neurological Institute.

to the most posterior regions (Figure 2, lower row). As shown in the lower rows of Figure 5A and B, this region has the highest overlap with the pulvinar nucleus. This nucleus also belongs to the higher-order thalamic nuclei and has extensive connections to several cortices, including the temporal, prefrontal, and visual cortices (71,72). In addition, the pulvinar nucleus is the thalamic nucleus that has been most consistently reported to have structural alterations in postmortem investigations of schizophrenia (22). Consistent with this finding, we found microstructural changes in this region, which may have effects on information flow and filtering. As stated above, this result also aligned well with previous reports of thalamocortical alterations, as the pulvinar nucleus has extensive cortical connections.

The temporal cortex is responsible for sensory processing (73), and this cortex is one of the regions that has been highlighted in schizophrenia for structural and functional alterations (74–79). Microstructural alterations within the tightly connected thalamic region suggest the involvement of malfunctions in relaying and controlling signals.

In the supplementary analysis, this region exhibited no significant reduction in thalamocortical connectivity, but the MK and thalamocortical connectivity were coupled in HCs in such a way that lower thalamocortical connectivity was compensated for by denser microstructural developments of the nuclei, possibly allowing for less the thalamocortical connections during development. This coupling was missing in the patients with FEP, which was speculated to be due to the reduction in the microstructural complexity that occurred after the establishment of the thalamo-LTC connection. As it is only a speculation, further studies with longitudinal designs would aid in the understanding of this complex relationship between the microstructure and the thalamocortical connectivity and the role of this relationship in the pathophysiology of schizophrenia.

Diffusion Kurtosis Imaging

While this is, to the best of our knowledge, the first study to look at diffusion kurtosis in the gray matter of patients with FEP, one previous study reported widespread abnormalities in white matter kurtosis in schizophrenia (80). Going a step further than the white matter approach, our results showed that this measure of kurtosis successfully detected changes in the thalamus. As thalamic development begins early in the embryonic stage (81), neurodevelopmental alterations that diminish changes in macromolecule concentration and cell packing density from early life are speculated to cause this change; this speculation aligns with the neurodevelopmental hypothesis of schizophrenia (82).

However, there was no direct correlation between the MKs of in the thalamic nuclei and clinical scores. Similar to the thalamocortical connections or auditory oddball findings without any symptomatic correlation (14,83,84), the microstructure in these regions may not be linearly linked to the symptoms. It is speculated that alterations in the thalamic microstructure may cause complex cascades that are defective as well as compensatory, leading to a nonlinear relationship to the symptoms.

Limitations

Many of the patients with FEP in this study were on antipsychotics at the time of the scanning. Although the effects would be relatively small in patients with FEP compared with those in patients with chronic schizophrenia, antipsychotics and antidepressants are reported to have subtle but measurable impacts on generalized and specific brain tissues (85,86).

In the connectivity-based segmentation of the thalamus, the cortical ROIs were chosen based on previously reported thalamocortical connection studies (17,50) to reference their results of altered connectivity with the findings in this study. However, using different cortical ROIs in the connectivity-based segmentation would have resulted in different patterns of segmentation; this fact remains a limitation of this study (two-way ANCOVA results of the groups and thalamic segments are included regarding this issue and are discussed in the Supplement).

Also, the correlation between SWM and OFC MK in FEP must be interpreted with caution, as it is uncorrected for the multiple neurocognitive test comparisons.

The single B0-image acquisition and nonisotropic voxel shape were also possible limitations of the image acquisition. In particular, the long voxel shapes in the z-axis might have affected the fiber reconstruction slightly differently depending on the fiber orientation, which might have caused changes in the segmentation pattern. Additionally, the susceptibility artifact could have been improved using techniques such as field mapping or dual-diffusion acquisition encoding directions.

Conclusions

Reduced MKs in the thalamic regions corresponding to the mediodorsal and pulvinar nuclei in patients with FEP highlight the existence of nuclei-specific thalamic anomalies in the early course of schizophrenia. The multimodal approach employed in this study allowed more detailed and more individualized segmentation of the thalamic nuclei, and the results from our analysis suggested that thalamic microstructural changes may be important biomarkers of psychosis that can be used for early detection, and possibly early intervention, for schizophrenia.

ACKNOWLEDGMENTS AND DISCLOSURES

This research was supported by the Brain Research Program through the National Research Foundation of Korea funded by the Ministry of Science, Information and Communication Technologies, and Future Planning (Grant No. 2017M3C7A1029610 [to JSK]). The authors report no biomedical financial interests or potential conflicts of interest.

ARTICLE INFORMATION

From the Institute of Human Behavioral Medicine (KIKC, TYL, JSK), Seoul National University Medical Research Center; Department of Brain and Cognitive Sciences (KIKC, YBK, WJH, JSK), College of Natural Sciences; and Department of Psychiatry (JL, MK, TYL, JSK), College of Medicine, Seoul National University, Seoul, Republic of Korea.

Address correspondence to Jun Soo Kwon, M.D., Ph.D., Department of Psychiatry, College of Medicine and Department of Brain and Cognitive Sciences, College of Natural Science, Seoul National University, 101 Daehak-no, Jongno-gu, Seoul 110–744, Republic of Korea; E-mail: kwonjs@snu.ac.kr.

Received Dec 7, 2017; revised and accepted May 21, 2018.

Supplementary material cited in this article is available online at https://doi.org/10.1016/j.biopsych.2018.05.019.

REFERENCES

1. Pakkenberg B (1990): Pronounced reduction of total neuron number in mediodorsal thalamic nucleus and nucleus accumbens in schizophrenics. Arch Gen Psychiatry 47:1023–1028.
2. Bogerts B (1993): Recent advances in the neuropathology of schizophrenia. Schizophr Bull 19:431–445.
3. Andreasen NC, Ehrhardt JC, Swayze VW 2nd, Alliger RJ, Yuh WT, Cohen G, *et al.* (1990): Magnetic resonance imaging of the brain in schizophrenia. The pathophysiologic significance of structural abnormalities. Arch Gen Psychiatry 47:35–44.
4. Flaum M, Swayze VW 2nd, O'Leary DS, Yuh WT, Ehrhardt JC, Arndt SV, *et al.* (1995): Effects of diagnosis, laterality, and gender on brain morphology in schizophrenia. Am J Psychiatry 152:704–714.
5. Adriano F, Spoletini I, Caltagirone C, Spalletta G (2010): Updated meta-analyses reveal thalamus volume reduction in patients with first-episode and chronic schizophrenia. Schizophr Res 123:1–14.
6. Haijma SV, Van Haren N, Cahn W, Koolschijn PC, Hulshoff Pol HE, Kahn RS (2013): Brain volumes in schizophrenia: A meta-analysis in over 18 000 subjects. Schizophr Bull 39:1129–1138.
7. Watis L, Chen SH, Chua HC, Chong SA, Sim K (2008): Glutamatergic abnormalities of the thalamus in schizophrenia: A systematic review. J Neural Transm (Vienna) 115:493–511.
8. Martins-de-Souza D, Maccarrone G, Wobrock T, Zerr I, Gormanns P, Reckow S, *et al.* (2010): Proteome analysis of the thalamus and cerebrospinal fluid reveals glycolysis dysfunction and potential biomarkers candidates for schizophrenia. J Psychiatr Res 44:1176–1189.
9. Andreasen NC, O'Leary DS, Cizadlo T, Arndt S, Rezai K, Ponto LL, *et al.* (1996): Schizophrenia and cognitive dysmetria: A positron-emission tomography study of dysfunctional prefrontal-thalamic-cerebellar circuitry. Proc Natl Acad Sci U S A 93:9985–9990.
10. Hazlett EA, Buchsbaum MS, Byne W, Wei TC, Spiegel-Cohen J, Geneve C, *et al.* (1999): Three-dimensional analysis with MRI and PET of the size, shape, and function of the thalamus in the schizophrenia spectrum. Am J Psychiatry 156:1190–1199.
11. Heckers S, Curran T, Goff D, Rauch SL, Fischman AJ, Alpert NM, *et al.* (2000): Abnormalities in the thalamus and prefrontal cortex during episodic object recognition in schizophrenia. Biol Psychiatry 48:651–657.
12. Tregellas JR, Davalos DB, Rojas DC, Waldo MC, Gibson L, Wylie K, *et al.* (2007): Increased hemodynamic response in the hippocampus, thalamus and prefrontal cortex during abnormal sensory gating in schizophrenia. Schizophr Res 92:262–272.
13. Andreasen NC (1997): The role of the thalamus in schizophrenia. Can J Psychiatry 42:27–33.
14. Woodward ND, Karbasforoushan H, Heckers S (2012): Thalamocortical dysconnectivity in schizophrenia. Am J Psychiatry 169:1092–1099.
15. Kubota M, Miyata J, Sasamoto A, Sugihara G, Yoshida H, Kawada R, *et al.* (2013): Thalamocortical disconnection in the orbitofrontal region associated with cortical thinning in schizophrenia. JAMA Psychiatry 70:12–21.
16. Anticevic A, Haut K, Murray JD, Repovs G, Yang GJ, Diehl C, *et al.* (2015): Association of thalamic dysconnectivity and conversion to psychosis in youth and young adults at elevated clinical risk. JAMA Psychiatry 72:882–891.
17. Cho KI, Shenton ME, Kubicki M, Jung WH, Lee TY, Yun JY, *et al.* (2015): Altered thalamo-cortical white matter connectivity: probabilistic tractography study in clinical-high risk for psychosis and first-episode psychosis. Schizophr Bull 42:723–731.
18. Woodward ND, Heckers S (2016): Mapping Thalamocortical Functional Connectivity in Chronic and Early Stages of Psychotic Disorders. Biol Psychiatry 79:1016–1025.
19. Giraldo-Chica M, Rogers BP, Damon SM, Landman BA, Woodward ND (2018): Prefrontal-Thalamic Anatomical Connectivity and Executive Cognitive Function in Schizophrenia. Biol Psychiatry 83:509–517.
20. Ferri J, Ford JM, Roach BJ, Turner JA, van Erp TG, Voyvodic J, *et al.* (2018): Resting-state thalamic dysconnectivity in schizophrenia and relationships with symptoms. Psychol Med 15:1–8.
21. Jones EG (2007): The Thalamus, 2nd ed. Cambridge, United Kingdom: Cambridge University Press.
22. Dorph-Petersen KA, Lewis DA (2017): Postmortem structural studies of the thalamus in schizophrenia. Schizophr Res 180:28–35.
23. Bogerts B, Meertz E, Schonfeldt-Bausch R (1985): Basal ganglia and limbic system pathology in schizophrenia. A morphometric study of brain volume and shrinkage. Arch Gen Psychiatry 42:784–791.
24. Byne W, Fernandes J, Haroutunian V, Huacon D, Kidkardnee S, Kim J, *et al.* (2007): Reduction of right medial pulvinar volume and neuron number in schizophrenia. Schizophr Res 90:71–75.
25. Byne W, Buchsbaum MS, Mattiace LA, Hazlett EA, Kemether E, Elhakem SL, *et al.* (2002): Postmortem assessment of thalamic nuclear volumes in subjects with schizophrenia. Am J Psychiatry 159:59–65.
26. Mitchell AS, Browning PG, Wilson CR, Baxter MG, Gaffan D (2008): Dissociable roles for cortical and subcortical structures in memory retrieval and acquisition. J Neurosci 28:8387–8396.
27. Snow JC, Allen HA, Rafal RD, Humphreys GW (2009): Impaired attentional selection following lesions to human pulvinar: Evidence for homology between human and monkey. Proc Natl Acad Sci U S A 106:4054–4059.
28. Wilke M, Turchi J, Smith K, Mishkin M, Leopold DA (2010): Pulvinar inactivation disrupts selection of movement plans. J Neurosci 30:8650–8659.
29. Purushothaman G, Marion R, Li K, Casagrande VA (2012): Gating and control of primary visual cortex by pulvinar. Nat Neurosci 15:905–912.
30. Theyel BB, Llano DA, Sherman SM (2010): The corticothalamocortical circuit drives higher-order cortex in the mouse. Nat Neurosci 13:84–88.
31. Csernansky JG, Schindler MK, Splinter NR, Wang L, Gado M, Selemon LD, *et al.* (2004): Abnormalities of thalamic volume and shape in schizophrenia. Am J Psychiatry 161:896–902.
32. Janssen J, Aleman-Gomez Y, Reig S, Schnack HG, Parellada M, Graell M, *et al.* (2012): Regional specificity of thalamic volume deficits in male adolescents with early-onset psychosis. Br J Psychiatry 200:30–36.
33. Kemether EM, Buchsbaum MS, Byne W, Hazlett EA, Haznedar M, Brickman AM, *et al.* (2003): Magnetic resonance imaging of mediodorsal, pulvinar, and centromedian nuclei of the thalamus in patients with schizophrenia. Arch Gen Psychiatry 60:983–991.
34. Behrens TE, Johansen-Berg H, Woolrich MW, Smith SM, Wheeler-Kingshott CA, Boulby PA, *et al.* (2003): Non-invasive mapping of connections between human thalamus and cortex using diffusion imaging. Nat Neurosci 6:750–757.
35. Johansen-Berg H, Behrens TE, Sillery E, Ciccarelli O, Thompson AJ, Smith SM, *et al.* (2005): Functional-anatomical validation and individual variation of diffusion tractography-based segmentation of the human thalamus. Cereb Cortex 15:31–39.
36. Ji B, Li Z, Li K, Li L, Langley J, Shen H, *et al.* (2016): Dynamic thalamus parcellation from resting-state fMRI data. Hum Brain Mapp 37:954–967.
37. Kim JJ, Kim DJ, Kim TG, Seok JH, Chun JW, Oh MK, *et al.* (2007): Volumetric abnormalities in connectivity-based subregions of the thalamus in patients with chronic schizophrenia. Schizophr Res 97:226–235.
38. Jensen JH, Helpern JA (2010): MRI quantification of non-Gaussian water diffusion by kurtosis analysis. NMR Biomed 23:698–710.
39. Delgado y Palacios R, Verhoye M, Henningsen K, Wiborg O, Van der Linden A (2014): Diffusion kurtosis imaging and high-resolution MRI demonstrate structural aberrations of caudate putamen and amygdala after chronic mild stress. PLoS One 9:e95077.
40. Delgado y Palacios R, Campo A, Henningsen K, Verhoye M, Poot D, Dijkstra J, *et al.* (2011): Magnetic resonance imaging and spectroscopy reveal differential hippocampal changes in anhedonic and

resilient subtypes of the chronic mild stress rat model. Biol Psychiatry 70:449–457.
41. Steven AJ, Zhuo J, Melhem ER (2014): Diffusion kurtosis imaging: An emerging technique for evaluating the microstructural environment of the brain. AJR Am J Roentgenol 202:W26–W33.
42. Cheung MM, Hui ES, Chan KC, Helpern JA, Qi L, Wu EX (2009): Does diffusion kurtosis imaging lead to better neural tissue characterization? A rodent brain maturation study. Neuroimage 45:386–392.
43. Paydar A, Fieremans E, Nwankwo JI, Lazar M, Sheth HD, Adisetiyo V, *et al.* (2014): Diffusional kurtosis imaging of the developing brain. AJNR Am J Neuroradiol 35:808–814.
44. Woods SW (2003): Chlorpromazine equivalent doses for the newer atypical antipsychotics. J Clin Psychiatry 64:663–667.
45. Kay SR, Fiszbein A, Opler LA (1987): The positive and negative syndrome scale (PANSS) for schizophrenia. Schizophr Bull 13:261–276.
46. Hall RC (1995): Global assessment of functioning. A modified scale. Psychosomatics 36:267–275.
47. Lee YS, Kim ZS (1995): Validity of short forms of the Korean-Wechsler Adult Intelligence Scale [in Korean]. Korean J Clin Psychol 14:111–116.
48. Golden CJ, Espe-Pfeifer P, Wachsler-Felder J (2000): Neuropsychological Interpretation of Objective Psychological Tests. New York, NY: Springer US.
49. Reuter M, Schmansky NJ, Rosas HD, Fischl B (2012): Within-subject template estimation for unbiased longitudinal image analysis. Neuroimage 61:1402–1418.
50. Marenco S, Stein JL, Savostyanova AA, Sambataro F, Tan HY, Goldman AL, *et al.* (2012): Investigation of anatomical thalamo-cortical connectivity and FMRI activation in schizophrenia. Neuropsychopharmacology 37:499–507.
51. Smith SM (2002): Fast robust automated brain extraction. Hum Brain Mapp 17:143–155.
52. Jenkinson M, Bannister P, Brady M, Smith S (2002): Improved optimization for the robust and accurate linear registration and motion correction of brain images. Neuroimage 17:825–841.
53. Jenkinson M, Smith S (2001): A global optimisation method for robust affine registration of brain images. Med Image Anal 5:143–156.
54. Behrens TE, Berg HJ, Jbabdi S, Rushworth MF, Woolrich MW (2007): Probabilistic diffusion tractography with multiple fibre orientations: What can we gain? Neuroimage 34:144–155.
55. Jenkinson M, Beckmann CF, Behrens TE, Woolrich MW, Smith SM (2012): FSL. Neuroimage 62:782–790.
56. Tabesh A, Jensen JH, Ardekani BA, Helpern JA (2011): Estimation of tensors and tensor-derived measures in diffusional kurtosis imaging. Magn Reson Med 65:823–836.
57. Lancaster JL, Rainey LH, Summerlin JL, Freitas CS, Fox PT, Evans AC, *et al.* (1997): Automated labeling of the human brain: A preliminary report on the development and evaluation of a forward-transform method. Hum Brain Mapp 5:238–242.
58. R Core Team (2013): R: A Language and Environment for Statistical Computing. Vienna, Austria: R Foundation for Statistical Computing.
59. Jones E, Oliphant T, Peterson P (2001): SciPy: Open source scientific tools for Python. Available at: http://www.scipy.org.
60. Pakkenberg B (1993): Leucotomized schizophrenics lose neurons in the mediodorsal thalamic nucleus. Neuropathol Appl Neurobiol 19:373–380.
61. Young KA, Manaye KF, Liang C, Hicks PB, German DC (2000): Reduced number of mediodorsal and anterior thalamic neurons in schizophrenia. Biol Psychiatry 47:944–953.
62. Ferrarelli F, Huber R, Peterson MJ, Massimini M, Murphy M, Riedner BA, *et al.* (2007): Reduced sleep spindle activity in schizophrenia patients. Am J Psychiatry 164:483–492.
63. Ferrarelli F, Tononi G (2017): Reduced sleep spindle activity point to a TRN-MD thalamus-PFC circuit dysfunction in schizophrenia. Schizophr Res 180:36–43.
64. Wamsley EJ, Tucker MA, Shinn AK, Ono KE, McKinley SK, Ely AV, *et al.* (2012): Reduced sleep spindles and spindle coherence in schizophrenia: Mechanisms of impaired memory consolidation? Biol Psychiatry 71:154–161.
65. Takayanagi Y, Takahashi T, Orikabe L, Masuda N, Mozue Y, Nakamura K, *et al.* (2010): Volume reduction and altered sulco-gyral pattern of the orbitofrontal cortex in first-episode schizophrenia. Schizophr Res 121:55–65.
66. Schultz CC, Koch K, Wagner G, Roebel M, Schachtzabel C, Gaser C, *et al.* (2010): Reduced cortical thickness in first episode schizophrenia. Schizophr Res 116:204–209.
67. Bartholomeusz CF, Whittle SL, Montague A, Ansell B, McGorry PD, Velakoulis D, *et al.* (2013): Sulcogyral patterns and morphological abnormalities of the orbitofrontal cortex in psychosis. Prog Neuropsychopharmacol Biol Psychiatry 44:168–177.
68. Cavada C, Schultz W (2000): The mysterious orbitofrontal cortex. Foreword. Cereb Cortex 10:205.
69. Hallock HL, Wang A, Griffin AL (2016): Ventral midline thalamus is critical for hippocampal-prefrontal synchrony and spatial working memory. J Neurosci 36:8372–8389.
70. Griffin AL (2015): Role of the thalamic nucleus reuniens in mediating interactions between the hippocampus and medial prefrontal cortex during spatial working memory. Front Syst Neurosci 9:29.
71. Bender DB (1981): Retinotopic organization of macaque pulvinar. J Neurophysiol 46:672–693.
72. Benevento LA, Standage GP (1983): The organization of projections of the retinorecipient and nonretinorecipient nuclei of the pretectal complex and layers of the superior colliculus to the lateral pulvinar and medial pulvinar in the macaque monkey. J Comp Neurol 217:307–336.
73. Heffner HE, Heffner RS (1984): Temporal lobe lesions and perception of species-specific vocalizations by macaques. Science 226:75–76.
74. Chun S, Westmoreland JJ, Bayazitov IT, Eddins D, Pani AK, Smeyne RJ, *et al.* (2014): Specific disruption of thalamic inputs to the auditory cortex in schizophrenia models. Science 344:1178–1182.
75. Crossley NA, Mechelli A, Fusar-Poli P, Broome MR, Matthiasson P, Johns LC, *et al.* (2009): Superior temporal lobe dysfunction and frontotemporal dysconnectivity in subjects at risk of psychosis and in first-episode psychosis. Hum Brain Mapp 30:4129–4137.
76. Yoon YB, Yun JY, Jung WH, Cho KI, Kim SN, Lee TY, *et al.* (2015): Altered fronto-temporal functional connectivity in individuals at ultra-high-risk of developing psychosis. PLoS One 10:e0135347.
77. Parker EM, Sweet RA (2017): Stereological assessments of neuronal pathology in auditory cortex in schizophrenia. Front Neuroanat 11:131.
78. Javitt DC, Sweet RA (2015): Auditory dysfunction in schizophrenia: Integrating clinical and basic features. Nat Rev Neurosci 16:535–550.
79. Kwon JS, O'Donnell BF, Wallenstein GV, Greene RW, Hirayasu Y, Nestor PG, *et al.* (1999): Gamma frequency-range abnormalities to auditory stimulation in schizophrenia. Arch Gen Psychiatry 56:1001–1005.
80. Zhu J, Zhuo C, Qin W, Wang D, Ma X, Zhou Y, *et al.* (2015): Performances of diffusion kurtosis imaging and diffusion tensor imaging in detecting white matter abnormality in schizophrenia. Neuroimage Clin 7:170–176.
81. Kostovic I, Judas M (2010): The development of the subplate and thalamocortical connections in the human foetal brain. Acta Paediatr 99:1119–1127.
82. Fatemi SH, Folsom TD (2009): The neurodevelopmental hypothesis of schizophrenia, revisited. Schizophr Bull 35:528–548.
83. Anticevic A, Cole MW, Repovs G, Murray JD, Brumbaugh MS, Winkler AM, *et al.* (2014): Characterizing thalamo-cortical disturbances in schizophrenia and bipolar illness. Cereb Cortex 24:3116–3130.
84. Kiehl KA, Stevens MC, Celone K, Kurtz M, Krystal JH (2005): Abnormal hemodynamics in schizophrenia during an auditory oddball task. Biol Psychiatry 57:1029–1040.
85. Geerlings MI, Brickman AM, Schupf N, Devanand DP, Luchsinger JA, Mayeux R, *et al.* (2012): Depressive symptoms, antidepressant use, and brain volumes on MRI in a population-based cohort of old persons without dementia. J Alzheimers Dis 30:75–82.
86. Ho BC, Andreasen NC, Ziebell S, Pierson R, Magnotta V (2011): Long-term antipsychotic treatment and brain volumes: A longitudinal study of first-episode schizophrenia. Arch Gen Psychiatry 68:128–137.